frontiers in Materials

MINI REVIEW
published: 12 April 2019
doi: 10.3389/fmats.2019.00057

High-Performance Perovskite Solar Cells Based on Low-Temperature Processed Electron Extraction Layer

Shun-Hsiang Chan[1], *Yin-Hsuan Chang*[1] *and Ming-Chung Wu*[1,2,3]*

[1] Department of Chemical and Materials Engineering, Chang Gung University, Taoyuan, Taiwan, [2] Green Technology Research Center, Chang Gung University, Taoyuan, Taiwan, [3] Division of Neonatology, Department of Pediatrics, Chang Gung Memorial Hospital, Taoyuan, Taiwan

Organic-inorganic perovskite solar cells (PSCs) is considered one of the most promising energy harvesting technologies due to its high power conversion efficiency (PCE). The T. Miyasaka group first reported the methylammonium lead halide ($CH_3NH_3PbX_3$) as a light absorber of dye-sensitized solar cells with a PCE of 3.8% in 2009. Over the past decade, many research groups have been dedicated to constructing high-performance PSCs and have obtained fantastic progress. Before commercialization, many issues have to be overcome. To extend the application of PSCs, flexible PSCs are seen as the preferred choice. However, the conventional process requires high-temperature procedures that are incompatible with the production of flexible PSCs. Here, we specifically focus on the recent developments of the low-temperature process strategies for fabricating high-performance PSCs. This mini-review briefly discusses the development in low-temperature processed metal oxide and carbon-based electron extraction layer (EEL). The approaches for low-temperature solution-processed PSCs are introduced and then the various PSCs with distinctive EEL are discussed. Overall, this mini-review contributes to a better understanding of the low-temperature processed electron extraction layer. Strategies and perspectives are also provided for further high-performance PSCs.

Keywords: perovskite solar cell, low-temperature process, electron extraction layer, metal oxide, power conversion efficiency

OPEN ACCESS

Edited by:
Liming Dai,
Case Western Reserve University,
United States

Reviewed by:
Lola González-García,
Leibniz Institut für Neue Materialien (LG), Germany
Josep Albero,
Instituto de Tecnología Química (ITQ), Spain

***Correspondence:**
Ming-Chung Wu
mingchungwu@cgu.edu.tw

Specialty section:
This article was submitted to Translational Materials Science, a section of the journal Frontiers in Materials

Received: *06 December 2018*
Accepted: *20 March 2019*
Published: *12 April 2019*

Citation:
Chan S-H, Chang Y-H and Wu M-C (2019) High-Performance Perovskite Solar Cells Based on Low-Temperature Processed Electron Extraction Layer. Front. Mater. 6:57. doi: 10.3389/fmats.2019.00057

INTRODUCTION

The issue of energy crisis has received increasing attention in recent years. Researchers from all over the world have been focusing on the development of renewable energy, such as wind, geothermal, biomass, and solar energy, etc. Solar energy is less costly among renewable energy, it is predictable compared with wind energy, and is less site-dependent. Hence, solar energy technology has flourished in recent years. From first-generation poly/monocrystalline silicon solar cell, second-generation thin-film solar cell to third-generation solution-processed solar cell, the manufacturing cost has been significantly reduced. Third-generation solution-processed solar cells include organic photovoltaic (OPV), dye-sensitized solar cell (DSSC), and perovskite solar cell (PSC). Currently, PSC exhibits a power conversion efficiency (PCE) of as high as 23.7% in 2019. The typical perovskite structure is ABX_3, where A is a monovalent cation [e.g., methylammonium (MA), formamidinium (FA), cesium (Cs), and rubidium (Rb)], B is a divalent cation [e.g., lead (Pb) and tin (Sn)], and X is a halide [e.g., chlorine (Cl), bromine (Br), and iodine (I)] (Liu et al., 2016; Saliba et al., 2016a,b).

Furthermore, the structure is based on A-site cation occupying a cuboctahedral site with BX_6 octahedra. The octahedron will connect with each other, and the center of each octahedron is the location of A cation. The PSC structure can be divided into two types, including p-i-n and n-i-p structures (**Figures 1A,B**). The p-i-n structured PSC is based on the organic solar cells having ITO/p-type material (HTL)/perovskite/n-type material (EEL)/metal electrode (Heo et al., 2015; Fan et al., 2018; Mali et al., 2018). In contrast, n-i-p structured PSC is adopted to construct DSSC with structure FTO/n-type material (EEL)/perovskite/p-type material (HTL)/metal electrode (Chan et al., 2017; Wu et al., 2018a). Many n-type materials, including TiO_2, Al_2O_3, ZnO, ZrO_2, and SnO_2, are often used as electron extraction layer (EEL) for PSC due to the appropriate energy band alignment with perovskite absorber (Anaraki et al., 2016; Che et al., 2016; Zhang et al., 2017, 2018; Wu et al., 2018a). However, the synthesis of metal oxides often requires high-temperature treatment to increase the crystallinity. Therefore, developing metal oxides for EEL through the low-temperature process is imperative. For the flexible PSC, the processing temperature is usually lower than 150°C. The low-temperature process can effectively reduce production cost and increase the feasibility of mass-production (e.g., roll-to-roll manufacturing) (Dou et al., 2018). The photovoltaic characteristic of PSC based on various EELs prepared by the low-temperature process are shown in **Table 1**. In this mini-review, we briefly introduce the development of the low-temperature processed metal oxide and carbon-based EEL for state-of-the-art PSC. Moreover, we also compared the PSC made by the high-temperature process to the ones made by the low-temperature process.

LOW-TEMPERATURE TiO_2 ELECTRON EXTRACTION LAYER

For n-i-p structured perovskite device, TiO_2 is often used as EEL due to the chemical stability, low-cost, and high charge transportability (**Figure 1C**). The minimum conduction band of TiO_2 is lower than that of perovskite absorber, so that the electron can be effectively transported from perovskite absorber to TiO_2 EEL. Moreover, the maximum valence band of TiO_2 is also lower than that of perovskite absorber, resulting in the excellent hole blocking capability (Wu et al., 2016). For the TiO_2-based EEL, it can be classified into two types, mesoporous-structured TiO_2 layer and TiO_2 compact layer (Wu et al., 2018b; Chen et al., 2019). The mesoporous-structured TiO_2 layer must be calcined at above 400°C to remove the organic binder (e.g., ethyl cellulose) and form the porous structure (Wu et al., 2018a). However, the high-temperature calcination leads to cost increment and energy consumption, and it is not conducive to the low-temperature process. Therefore, the low-temperature process to prepare the nanostructure TiO_2 layer has been regarded as a breakthrough. The low-temperature processed TiO_2 as the EEL of PSC can be prepared by pulsed laser deposition. A laser beam was used to sublime a TiO_2 target. Subsequently, the sublimed TiO_2 films were deposited onto an ITO substrate at 300°C. The hierarchical TiO_2 nanostructures can effectively increase the contact area with perovskite absorber. Therefore, the interface between hierarchical TiO_2 EEL/perovskite absorber exhibits high electron-hole pair separation and electron extraction behavior. The PSC based on hierarchical TiO_2 EEL has demonstrated a PCE of 14.1% (Yang et al., 2016).

The low-temperature processed 3D flower-like TiO_2 array is also an alternative EEL for high-performance PSC. The TiO_2 array layer was deposited on an FTO substrate by chemical bath deposition method. In this process, the FTO glass was immersed in an 80°C $TiCl_3$/HCl solution for 4 to 10 h in a furnace. Subsequently, the TiO_2 array layer was washed and dried at 100°C for 2 h. The light-harvesting efficiency of the perovskite-coated TiO_2 array increases with increasing chemical bath deposition reaction time of the 3D flower-like TiO_2 array EEL. This is beneficial for obtaining a full coverage of the perovskite absorber layer. The flower-like TiO_2 nanorods is anatase phase, and it shows the high light-harvesting and low recombination rate. The PSCs based on flower-like TiO_2 nanorods EEL has shown a PCE of 15.7% with high reproducibility and less hysteresis (**Supplementary Figure 1A**) (Chen et al., 2016).

The pin-hole free compact TiO_2 can be coated on FTO substrate with high coverage by the vacuum electron beam evaporation technique. For the mesoporous TiO_2 layer, it was fabricated by spin-coating method, followed by a UV treatment for 200 min. UV irradiation is used to remove the organic binders to form mesoporous scaffold. This work uses a full low-temperature process to prepare compact TiO_2 and mesoporous TiO_2 layer. For J-V curve measurement, the champion device reached a stabilized efficiency of 18.2% under AM 1.5G solar simulator light (**Supplementary Figure 1A**). This research has carried all requirements for high-efficiency perovskite/silicon tandem cell with the full low-temperature process (Schulze et al., 2017).

The planar PSC fabricated by the low-temperature process can reach a PCE >20%. The deep trap states present at the perovskite absorber/EEL interface can hinder the photovoltaic performance. Many literatures have indicated that passivating the perovskite absorber/EEL interface can efficiently suppress deep trap states. Chlorine-capped TiO_2 EEL is able to reduce interface recombination at TiO_2/perovskite absorber interface. Chlorine-capped TiO_2 nanocrystals was fabricated by the modified non-hydrolytic sol-gel method. The precursor solution was spin-coated on FTO glass, then annealed in 150°C ambient air for 30 min. The chloride added into perovskite absorber can enhance grain boundary passivation in perovskite device. This type of planar PSC has exhibited a high PCE of 20.1% without J-V hysteresis (**Supplementary Figure 1A**) (Tan et al., 2017).

LOW-TEMPERATURE ZnO ELECTRON EXTRACTION LAYER

ZnO is a low-cost n-type semiconductor having a bandgap of 3.3 eV (Gaspar et al., 2017). ZnO can replace TiO_2 as an EEL for PSC due to its higher electron mobility and suitable energy structure. Also, ZnO has a beneficial conduction band position at 4.4 eV, which is lower than LUMO of perovskite absorber.

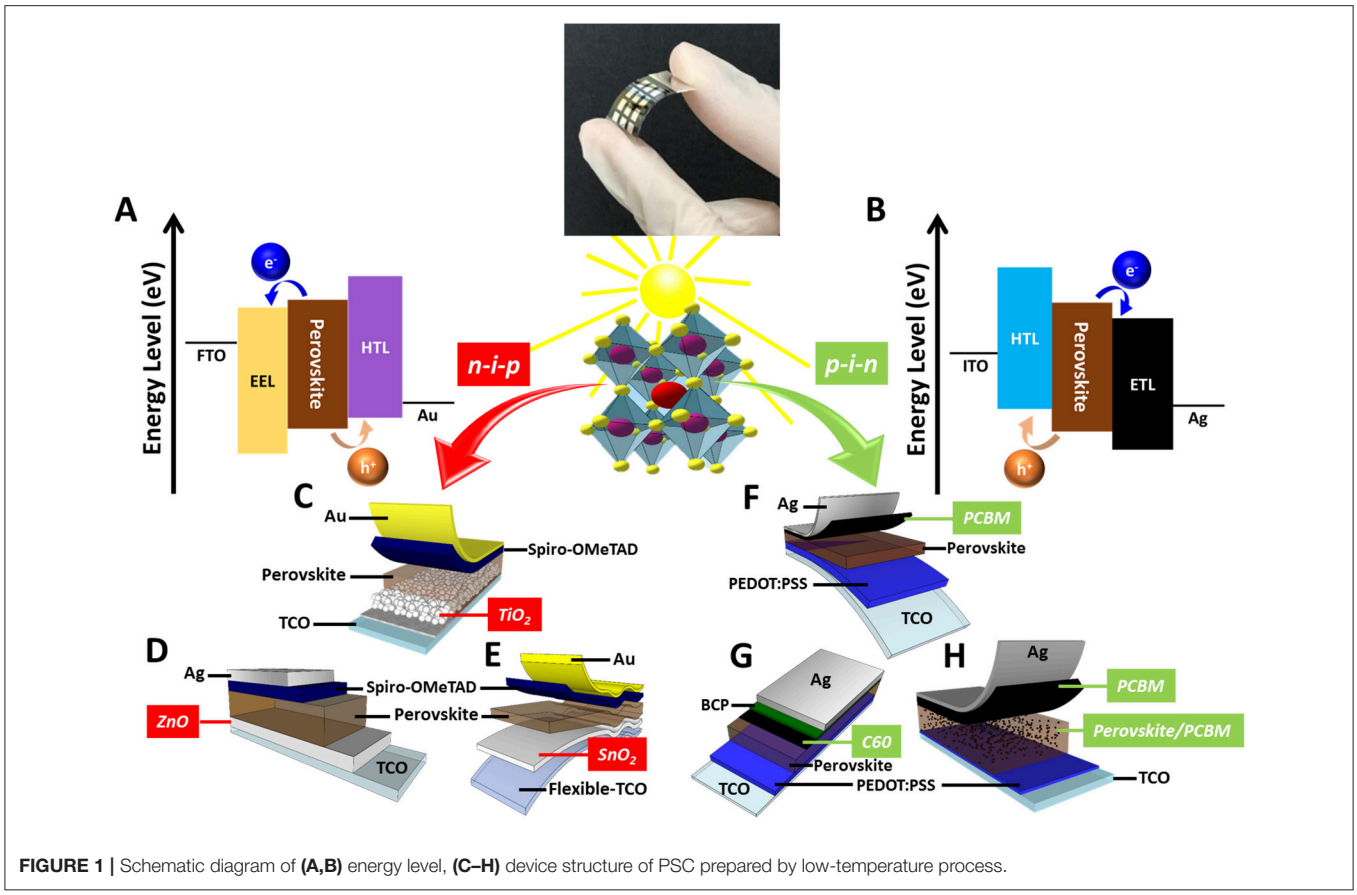

FIGURE 1 | Schematic diagram of **(A,B)** energy level, **(C–H)** device structure of PSC prepared by low-temperature process.

Therefore, ZnO has shown to play a critical role in improving the performance of PSC (Song et al., 2017). Especially, the fabricating temperature of ZnO film as EEL has been reduced to below 150°C (**Figure 1D**). The sol-gel ZnO was spin coated on ITO substrate, then annealed at 140°C. The optical property, surface morphology, and crystal structure of ZnO film can be tuned by adjusting thickness. The results have shown that the multi-layer ZnO film with high optical transmittance can increase the light absorption in perovskite absorber. After the thickness optimization of ZnO film, ZnO exhibits homogeneous surface morphology for the increment of perovskite crystal growth and suppression of deep trap states at the ZnO film/perovskite absorber interface. The PCE of PSC with ZnO film has reached 8.8% (**Supplementary Figure 1B**) (Mahmud et al., 2017).

To reduce the surface defects of the ZnO, chemical alkali-metal (Li, Na, and K) doping method has been adopted to passivate surface defect resulting in electron mobility enhancement and in raising the Fermi level. Doping metal ion into the semiconductor has been regarded as an effective strategy for electronic structure change. The alkali-metal doped ZnO EEL was prepared by dipping ZnO films into various 100°C alkali-metal hydroxide solutions for 10 min. Successfully doping alkali-metal ion into the low-temperature processed ZnO can simultaneously passivate surface defects. The performance of PSC with various alkali-metal doped ZnO EEL has shown to be higher than that with non-doped ZnO EEL. The PSC with K-doped ZnO EEL has achieved a PCE of 19.9% without significant J-V hysteresis (**Supplementary Figure 1B**) (Azmi et al., 2018).

LOW-TEMPERATURE SnO_2 ELECTRON EXTRACTION LAYER

J-V hysteresis in n-i-p planar PSC remains a challenge for the advancement of such material. The hysteresis can lead to misjudgment of photovoltaic performance because the forward and reverse scans show different results. Recently, SnO_2 has been reported as EEL of perovskite device that could eliminate J-V hysteresis in planar structure PSC due to its large bandgap (3.6 eV), higher electron mobility, optimal band alignment with perovskite absorber, and excellent electron extraction capability (Chen et al., 2018). SnO_2 has shown high conductivity without high-temperature calcination treatment, thus beneficial for the preparation of flexible PSC (**Figure 1E**).

For the band structure of SnO_2, it shows a lower conduction band and higher electron mobility compared to TiO_2 EEL. Tuning the band alignment between SnO_2 and perovskite absorber can facilitate charge transfer from perovskite absorber to SnO_2 EEL and reduce charge accumulation. Applying the low-temperature solution-processed SnO_2 as EEL can maintain high-performance for PSC. The SnO_2 precursor solution was prepared

TABLE 1 | List of state-of-the-art PSC based on EEL prepared by the low-temperature process.

Device structure	EEL	Processing temp. (°C)	Fabrication method	J_{sc} (mA/cm^2)	V_{oc} (volts)	FF (%)	PCE (%)	References
n-i-p	TiO_2	80	Chemical bath deposition	22.0	0.99	72.0	15.7	Chen et al., 2016
		120	Evaporation/UV Treatment	21.3	1.07	84.0	19.1	Schulze et al., 2017
		150	Spin-Coating	22.3	1.19	80.6	21.4	Tan et al., 2017
		300	Pulsed laser deposition	20.1	1.01	69.0	14.1	Yang et al., 2016
	ZnO	140	Spin-Coating	14.9	0.93	62.7	8.8	Mahmud et al., 2017
		130	Spin-Coating	23.0	1.13	77.1	19.9	Azmi et al., 2018
		150	Spin-Coating	22.6	1.11	75.3	18.9	Song et al., 2017
	SnO_2	150	Spin-Coating	24.9	1.09	75.7	20.5	Jiang et al., 2016
		≈RT	Spin-Coating /N_2 Plasma treatment	21.8	1.12	83.0	20.3	Subbiah et al., 2018
		180	Spin-Coating	21.9	1.13	78.0	19.4	Bu et al., 2018
		200	Atomic layer deposition	22.1	1.08	75.0	17.8	Kuang et al., 2018
	WO_x	150	Spin-Coating	21.8	0.71	58.0	9.0	Wang et al., 2015
	CeO_x	150	Spin-Coating	23.3	1.06	69.1	17.0	Wang et al., 2017b
	Nb_2O_5	≈RT	RF Magnetron sputtering technique	22.9	1.04	72.0	17.1	Ling et al., 2017
p-i-n	PCBM	100	Spin-Coating	21.8	1.04	78.0	17.8	Zhou et al., 2018
	PCBM (BHJ)	100	Spin-Coating	21.8	1.00	73.3	16.2	Chang et al., 2018
		100	Spin-Coating	20.2	0.97	82.0	16.0	Chiang and Wu, 2016
	C60	≈RT	Thermal evaporation	22.3	1.08	75.9	18.2	Liu et al., 2018

RT, room temperature; BHJ, bulk heterojunction; RF, radio frequency.

by diluting SnO_2 aqueous solution. The precursor solution was spin coated onto ITO substrates, then annealed on a 150°C hot plate for 30 min. SnO_2 EEL has been further constructed with the perovskite absorber by introducing an excess PbI_2 phase, passivating the traps in perovskite. This has achieved the best PCE of 20.5% without J-V hysteresis (**Supplementary Figure 1C**) (Jiang et al., 2016).

The low power nitrogen plasma treatment has been used to fabricate the low-temperature processed SnO_2 EEL. The SnO_2 precursor solution was prepared by dissolving $SnCl_4.5H_2O$ in IPA followed by continuous stirring for 2 h. The precursor solution was spin coated on rigid FTO or PET-ITO. Then, the samples were treated by low power RF plasma under nitrogen gas flow. Nitrogen plasma induces the initial cleavage of metal alkoxy and hydroxyl groups, resulting in the formation of the Sn-O-Sn framework. The PCE of PSC based on nitrogen plasma threated SnO_2 EEL has achieved 20.3% for rigid FTO substrates and 18.1% for flexible PSC (**Supplementary Figure 1C**) (Subbiah et al., 2018).

Atomic layer deposition is a deposition technique for high-quality film fabrication. Highly transparent amorphous SnO_2 was manufactured in atomic layer deposition reactor by low-temperature process (<200°C). The high-quality SnO_2 film exhibited high electron mobility (36 cm^2/V•s). The PCE of PSC with deposition temperature of 50 and 200°C SnO_2 has reached 17.5 and 17.8%, respectively (Kuang et al., 2018).

The PSC modules based on the low-temperature synthesized crystalline SnO_2 have been studied. The electron transport resistance of SnO_2 and charge recombination at EEL/perovskite absorber interface have been significantly decreased by thermal and UV-ozone treatments. The reported optimal thermal temperature for rigid PSC is 180°C, and can be decreased to 120°C for flexible PSC. The PCE of rigid PSC, flexible PSC, and 5 × 5 cm^2 flexible module have achieved 19.4, 16.5, and 12.4%, respectively (**Supplementary Figure 1C**) (Bu et al., 2018).

OTHER METAL OXIDE ELECTRON EXTRACTION LAYER

Tungsten oxide (WO_x) is n-type semiconductors with wide bandgap (2.0–3.0 eV) and high electron mobility (10–20 cm^2/V•s). These excellent properties make WO_x suitable as an EEL for perovskites photovoltaics. For the preparation of WO_x solution, tungsten hexachloride and n-propanol were mixed together, then the WO_x solution was spin coated on FTO. The amorphous WO_x EEL prepared by low-temperature solution process (150°C) shows higher electrical conductivity compared to TiO_2. Moreover, the excited electrons in perovskite absorber have shown to transfer more efficiently from perovskite absorber to WO_x EEL. Therefore, the short-circuit current density of PSC with WO_x EEL has shown to be higher than that of PSC with TiO_2 EEL. The PSC with WO_x EEL has shown an average PCE of 9.0% (**Supplementary Figure 1D**) (Wang et al., 2015).

Niobium oxide (Nb_2O_5) exhibits high electronic properties and high chemical stability. Therefore, Nb_2O_5 has also been seen as a candidate material for EEL. The amorphous Nb_2O_5 was fabricated at room temperature by a facile radio frequency magnetron sputtering technique on a Nb_2O_5 target in an argon atmosphere. The room-temperature sputtered Nb_2O_5 was successfully used as the EEL for planar PSC. The amorphous Nb_2O_5 film is highly transparent under visible region. As a

results, the PSC with the amorphous Nb_2O_5 EEL has exhibited a PCE of 17.2% (**Supplementary Figure 1D**) (Ling et al., 2017).

Cerium oxide (CeO_x) demonstrates wide bandgap, good transparency, large dielectric constant, and high chemical stability. CeO_x film was fabricated by sol-gel and spin-coating method at low temperature (150°C). The PSCs with CeO_x film showed high performance and high stability. Then the PCE of PSC with CeO_x film increased from 14.32 to 17.04% by [6,6]-phenyl C61 butyric acid methyl ester (PCBM) insertion (**Supplementary Figure 1D**) (Wang et al., 2017b).

FULLERENE COMPOUNDS ELECTRON EXTRACTION LAYER

The p-i-n structured PSC usually shows no hysteresis and is easier to prepare a flexible device. The p-i-n structured PSC has used [6,6]-phenyl C61 butyric acid methyl ester (PCBM) (**Supplementary Figure 2A**) (**Figure 1F**) and C60 (**Figure 1G**) as n-type EEL owing to its high electron mobility (Kuang et al., 2015). In order to further improve the PCE of the p-i-n structured PSC, the perovskite/PCBM heterojunction solar cell can be fabricated by a solvent engineering method (**Figure 1H**). The perovskite precursor solution contained PbI_2, $PbCl_2$, and CH_3NH_3I in DMSO/GBL solvent. PCBM solution was dissolved in chlorobenzene with various concentrations. After the perovskite precursor solution was spin coated on the substrate, the PCBM solution was injected on the perovskite film. The perovskite/PCBM films were annealed at 100°C for 20 min. The perovskite/PCBM heterojunction can improve the perovskite absorber quality and can increase charge extraction. Notably, adding PCBM during the baking procedure for perovskite absorber can form two separated EELs simultaneously, which effectively reduces the processing time. The champion device has exhibited a PCE of 17.8%, which is higher than that of the reference device (13.7%) (Zhou et al., 2018).

On the other hand, owing to the poor solubility of PCBM in DMF solvents, PCBM modification by fluorination can increase the solubility in the perovskite precursor. For the perovskite/fluorinated PCBM precursor solution, the fluorinated PCBM was directly added into the perovskite precursor solution. The perovskite/fluorinated PCBM precursor solution was spin coated on PEDOT:PSS film. The perovskite/fluorinated PCBM film was annealed at 100°C for 3 min to form the bulk heterojunction active layer. The fluorinated PCBM has shown to reduce the surface defects and to enhance the current density of PSC. The bulk heterojunction device with fluorinated PCBM has achieved a PCE of 16.2% with long-term stability (**Supplementary Figure 2B**) (Chang et al., 2018).

In order to enhance the fill factor of PSC, the perovskite-PCBM bulk heterojunction PSC has been fabricated by a low-temperature two-step spin-coating method. PCBM has been used as an acceptor to fill the vacancies and grain boundaries of the perovskite absorber. The product has demonstrated high current density, high fill factor, and high PCE because of high conductivity, high mobility, and long diffusion length of charge carriers. The bulk heterojunction PSC has achieved a PCE of 16.0%, fill factor of 82%, and without J-V hysteresis (Chiang and Wu, 2016).

Although fullerene compounds have been commonly used in p-i-n structured PSC, C60 has also been used as an EEL for p-i-n structured PSC recently. The C60 EEL with various thickness was deposited by vapor deposition in the evaporation chamber. Fluorescence microscopy and impedance spectroscopy have been used to investigate electron extraction behavior. The role of the C60 EEL can support electron extraction and collection. The PCE of PSC with 1 nm C60 EEL has achieved 18.0%. J-V hysteresis has also been significantly eliminated due to reduced space charge accumulation at the interface (**Supplementary Figure 2C**) (Liu et al., 2018).

ADVANTAGES AND DISADVANTAGES OF THE DIFFERENT APPROACHES

As mentioned above, most of the EEL is prepared by spin coating method due to easy fabrication, low-cost, and solution process. However, the spin coating method is very difficult when preparing a large-area film as the non-uniform film can directly affect device performance. The advantages of chemical bath deposition are a simple experimental setup and good reproducibility. But chemical bath deposition often requires a large amount of solution. Although evaporation and sputtering technique can produce large-area and uniform film, such methods require high vacuum and expensive equipment. Pulsed laser deposition can deposit many materials with the same composition as the target materials. Nevertheless, the coverage of the films is difficult to control by pulsed laser deposition. Atomic layer deposition can grow different multilayer structures with high sensitivity and precision. However, the disadvantages of atomic layer deposition are a longer process time for film fabrication and expensive setup. This summary also shows that the advantages and disadvantages of various methods should be considered for EEL fabrication.

CURRENT ISSUES AND FUTURE CHALLENGES FOR ELECTRON EXTRACTION LAYER

For the traditional high-temperature process, the EEL exhibits uniform mesoporous structure and high crystallinity. Comparing to the high-temperature process, the low-temperature process shows many fascinating advantages. The photovoltaic performance of PSC with the low-temperature process can still maintain high efficiency due to (1) passivation of the perovskite absorber/EEL interface, (2) high conductivity of EEL, and (3) application of UV or plasma treatment for EEL coalescence. Furthermore, the low-temperature processed EEL has shown to eliminate the hysteresis (Wojciechowski et al., 2014; Hou et al., 2015; Jeong et al., 2016; Tan et al., 2017; Wang et al., 2017a). When selecting EEL, several essential properties should be considered: (1) good electron mobility, (2) wide bandgap, and (3) band alignment with perovskite absorber. EEL with good electron mobility can facilitate the electron collection. For n-i-p

structured PSC, the wide bandgap EEL is selected to facilitate the absorption behavior of perovskite absorber. With the proper band alignment, it can promote electron transfer from perovskite active layer to EEL and can block holes to avoid recombination. If the above issues can all be satisfied and the existence of J-V hysteresis be eliminated, PSC with low-temperature process EEL can achieve a breakthrough in solar energy technology and realize commercialization.

CONCLUSIONS

In this mini-review, we summarized the metal oxide-based and fullerene compound-based EEL for PSC. Many n-type materials used for EEL, including TiO_2, ZnO, SnO_2, WO_x, CeO_x, Nb_2O_5, PCBM, and C60 have been thoroughly introduced. In addition, all these alternative materials for EEL can be fabricated under low-temperature process and can achieve PCE of over 20%. Using a low-temperature process to produce high-performance PSC is a major breakthrough. However, there are two issues that must be overcome before commercialization. The first one is the fast degradation phenomenon under humidity or constant irradiation, and the second is the hysteresis phenomena that can cause inaccurate estimation of PCE. The low-temperature process can effectively reduce production costs and energy waste. After addressing these issues, the commercialization of the low cost and flexible PSC is just around the corner.

AUTHOR CONTRIBUTIONS

S-HC wrote the submitted this mini-review. Y-HC revised and communicated the manuscript. M-CW supervised and wrote the manuscript.

ACKNOWLEDGMENTS

Financial support was obtained from Ministry of Science and Technology of Taiwan (Project Nos. 106-2221-E-182-057-MY3 and 107-2119-M-002-012), Chang Gung University (QZRPD181), and Chang Gung Memorial Hospital, Linkou (CMRPD2H0171 and BMRPC74) are highly appreciated.

SUPPLEMENTARY MATERIAL

The Supplementary Material for this article can be found online at: https://www.frontiersin.org/articles/10.3389/fmats.2019.00057/full#supplementary-material

REFERENCES

Anaraki, E. H., Kermanpur, A., Steier, L., Domanski, K., Matsui, T., Tress, W., et al. (2016). Highly efficient and stable planar perovskite solar cells by solution-processed tin oxide. *Energy Environ. Sci.* 9, 3128–3134. doi: 10.1039/C6EE02390H

Azmi, R., Hwang, S., Yin, W., Kim, T.-W., Ahn, T. K., and Jang, S.-Y. (2018). High efficiency low-temperature processed perovskite solar cells integrated with alkali metal doped ZnO electron transport layers. *ACS Energy Lett.* 3, 1241–1246. doi: 10.1021/acsenergylett.8b00493

Bu, T., Shi, S., Li, J., Liu, Y., Shi, J., Chen, L., et al. (2018). Low-temperature presynthesized crystalline tin oxide for efficient flexible perovskite solar cells and modules. *ACS Appl. Mater. Interfaces* 10, 14922–14929. doi: 10.1021/acsami.8b02624

Chan, S.-H., Wu, M.-C., Lee, K.-M., Chen, W.-C., Lin, T.-H., and Su, W.-F. (2017). Enhancing perovskite solar cell performance and stability by doping barium in methylammonium lead halide. *J. Mater. Chem. A* 5, 18044–18052. doi: 10.1039/C7TA05720B

Chang, C.-Y., Wang, C.-P., Raja, R., Wang, L., Tsao, C.-S., and Su, W.-F. (2018). High-efficiency bulk heterojunction perovskite solar cell fabricated by one-step solution process using single solvent: synthesis and characterization of material and film formation mechanism. *J. Mater. Chem. A* 6, 4179–4188. doi: 10.1039/C7TA07939G

Che, M., Zhu, L., Zhao, Y. L., Yao, D. S., Gu, X. Q., Song, J., et al. (2016). Enhancing current density of perovskite solar cells using TiO_2-ZrO_2 composite scaffold layer. *Mater. Sci. Semicond. Process.* 56, 29–36. doi: 10.1016/j.mssp.2016.07.003

Chen, S.-H., Chan, S.-H., Lin, Y.-T., and Wu, M.-C. (2019). Enhanced power conversion efficiency of perovskite solar cells based on mesoscopic Ag-doped TiO_2 electron transport layer. *Appl. Surf. Sci.* 469, 18–26. doi: 10.1016/j.apsusc.2018.10.256

Chen, X., Tang, L. J., Yang, S., Hou, Y., and Yang, H. G. (2016). A low-temperature processed flower-like TiO_2 array as an electron transport layer for high-performance perovskite solar cells. *J. Mater. Chem. A* 4, 6521–6526. doi: 10.1039/C6TA00893C

Chen, Y., Meng, Q., Zhang, L., Han, C., Gao, H., Zhang, Y., et al. (2018). SnO_2-based electron transporting layer materials for perovskite solar cells: a review of recent progress. *J. Energy Chem.* 35, 144–167. doi: 10.1016/j.jechem.2018.11.011

Chiang, C.-H., and Wu, C.-G. (2016). Bulk heterojunction perovskite-PCBM solar cells with high fill factor. *Nat. Photonics* 10, 196–200. doi: 10.1038/nphoton.2016.3

Dou, B., Whitaker, J. B., Bruening, K., Moore, D. T., Wheeler, L. M., Ryter, J., et al. (2018). Roll-to-roll printing of perovskite solar cells. *ACS Energy Lett.* 3, 2558–2565. doi: 10.1021/acsenergylett.8b01556

Fan, P., Zheng, D., Zheng, Y., and Yu, J. (2018). Efficient and stable planar p-i-n perovskite solar cells by doping tungsten compound into PEDOT:PSS to facilitate perovskite crystalline. *Electrochim. Acta* 283, 922–930. doi: 10.1016/j.electacta.2018.07.029

Gaspar, D., Pereira, L., Gehrke, K., Galler, B., Fortunato, E., and Martins, R. (2017). High mobility hydrogenated zinc oxide thin films. *Sol. Energy Mater. Sol. Cells* 163, 255–262. doi: 10.1016/j.solmat.2017.01.030

Heo, J. H., Han, H. J., Kim, D., Ahn, T. K., and Im, S. H. (2015). Hysteresis-less inverted $CH_3NH_3PbI_3$ planar perovskite hybrid solar cells with 18.1% power conversion efficiency. *Energy Environ. Sci.* 8, 1602–1608. doi: 10.1039/C5EE00120J

Hou, Y., Quiroz, C. O. R., Scheiner, S., Chen, W., Stubhan, T., Hirsch, A., et al. (2015). Low-temperature and hysteresis-free electron-transporting layers for efficient, regular, and planar structure perovskite solar cells. *Adv. Energy Mater.* 5:1501056. doi: 10.1002/aenm.201501056

Jeong, I., Jung, H., Park, M., Park, J. S., Son, H. J., Joo, J., et al. (2016). A tailored TiO_2 electron selective layer for high-performance flexible perovskite solar cells via low temperature UV process. *Nano Energy* 28, 380–389. doi: 10.1016/j.nanoen.2016.09.004

Jiang, Q., Zhang, L., Wang, H., Yang, X., Meng, J., Liu, H., et al. (2016). Enhanced electron extraction using SnO_2 for high-efficiency planar-structure $HC(NH_2)_2PbI_3$-based perovskite solar cells. *Nat. Energy* 2:16177. doi: 10.1038/nenergy.2016.177

Kuang, C., Tang, G., Jiu, T., Yang, H., Liu, H., Li, B., et al. (2015). Highly efficient electron transport obtained by doping PCBM with graphdiyne in planar-heterojunction perovskite solar cells. *Nano Lett.* 15, 2756–2762. doi: 10.1021/acs.nanolett.5b00787

Kuang, Y., Zardetto, V., Van Gils, R., Karwal, S., Koushik, D., Verheijen, M. A., et al. (2018). Low-temperature plasma-assisted atomic-layer-deposited SnO_2 as

an electron transport layer in planar perovskite solar cells. *ACS Appl. Mater. Interfaces* 10, 30367–30378. doi: 10.1021/acsami.8b09515

Ling, X., Yuan, J., Liu, D., Wang, Y., Zhang, Y., Chen, S., et al. (2017). Room-temperature processed Nb_2O_5 as the electron-transporting layer for efficient planar perovskite solar cells. *ACS Appl. Mater. Interfaces* 9, 23181–23188. doi: 10.1021/acsami.7b05113

Liu, D., Wang, Q., Traverse, C. J., Yang, C., Young, M., Kuttipillai, P. S., et al. (2018). Impact of ultrathin C60 on perovskite photovoltaic devices. *ACS Nano* 12, 876–883. doi: 10.1021/acsnano.7b08561

Liu, X., Yang, Z., Chueh, C.-C., Rajagopal, A., Williams, S. T., Sun, Y., et al. (2016). Improved efficiency and stability of Pb-Sn binary perovskite solar cells by Cs substitution. *J. Mater. Chem. A* 4, 17939–17945. doi: 10.1039/C6TA07712A

Mahmud, M. A., Elumalai, N. K., Upama, M. B., Wang, D., Chan, K. H., Wright, M., et al. (2017). Low temperature processed ZnO thin film as electron transport layer for efficient perovskite solar cells. *Sol. Energy Mater. Sol. Cells* 159, 251–264. doi: 10.1016/j.solmat.2016.09.014

Mali, S. S., Kim, H., Kim, H. H., Shim, S. E., and Hong, C. K. (2018). Nanoporous p-type NiOx electrode for p-i-n inverted perovskite solar cell toward air stability. *Mater. Today* 21, 483–500. doi: 10.1016/j.mattod.2017.12.002

Saliba, M., Matsui, T., Domanski, K., Seo, J.-Y., Ummadisingu, A., Zakeeruddin, S. M., et al. (2016a). Incorporation of rubidium cations into perovskite solar cells improves photovoltaic performance. *Science*. 354, 206–209. doi: 10.1126/science.aah5557

Saliba, M., Matsui, T., Seo, J.-Y., Domanski, K., Correa-Baena, J.-P., Nazeeruddin, M. K., et al. (2016b). Cesium-containing triple cation perovskite solar cells: improved stability, reproducibility and high efficiency. *Energy Environ. Sci.* 9, 1989–1997. doi: 10.1039/c5ee03874j

Schulze, P. S. C., Bett, A. J., Winkler, K., Hinsch, A., Lee, S., Mastroianni, S., et al. (2017). Novel low-temperature process for perovskite solar cells with a mesoporous TiO_2 scaffold. *ACS Appl. Mater. Interfaces* 9, 30567–30574. doi: 10.1021/acsami.7b05718

Song, J., Liu, L., Wang, X.-F., Chen, G., Tian, W., and Miyasaka, T. (2017). Highly efficient and stable low-temperature processed ZnO solar cells with triple cation perovskite absorber. *J. Mater. Chem. A* 5, 13439–13447. doi: 10.1039/C7TA03331A

Subbiah, A. S., Mathews, N., Mhaisalkar, S., and Sarkar, S. K. (2018). Novel plasma-assisted low-temperature-processed SnO_2 thin films for efficient flexible perovskite photovoltaics. *ACS Energy Lett.* 3, 1482–1491. doi: 10.1021/acsenergylett.8b00692

Tan, H., Jain, A., Voznyy, O., Lan, X., García De Arquer, F. P., Fan, J. Z., et al. (2017). Efficient and stable solution-processed planar perovskite solar cells via contact passivation. *Science* 355, 722–726. doi: 10.1126/science.aai9081

Wang, K., Shi, Y., Dong, Q., Li, Y., Wang, S., Yu, X., et al. (2015). Low-temperature and solution-processed amorphous WO_X as electron-selective layer for perovskite solar cells. *J. Phys. Chem. Lett.* 6, 755–759. doi: 10.1021/acs.jpclett.5b00010

Wang, L., Liu, F., Liu, T., Cai, X., Wang, G., Ma, T., et al. (2017a). Low-temperature processed compact layer for perovskite solar cells with negligible hysteresis. *Electrochim. Acta* 235, 640–645. doi: 10.1016/j.electacta.2017.03.145

Wang, X., Deng, L.-L., Wang, L.-Y., Dai, S.-M., Xing, Z., Zhan, X.-X., et al. (2017b). Cerium oxide standing out as an electron transport layer for efficient and stable perovskite solar cells processed at low temperature. *J. Mater. Chem. A* 5, 1706–1712. doi: 10.1039/C6TA07541J

Wojciechowski, K., Saliba, M., Leijtens, T., Abate, A., and Snaith, H. J. (2014). Sub-150°C processed meso-superstructured perovskite solar cells with enhanced efficiency. *Energy Environ. Sci.* 7, 1142–1147. doi: 10.1039/C3EE43707H

Wu, M.-C., Chan, S.-H., Jao, M.-H., and Su, W.-F. (2016). Enhanced short-circuit current density of perovskite solar cells using Zn-doped TiO_2 as electron transport layer. *Sol. Energy Mater. Sol. Cells* 157, 447–453. doi: 10.1016/j.solmat.2016.07.003

Wu, M.-C., Chan, S.-H., Lee, K.-M., Chen, S.-H., Jao, M.-H., Chen, Y.-F., et al. (2018a). Enhancing the efficiency of perovskite solar cells using mesoscopic zinc-doped TiO_2 as the electron extraction layer through band alignment. *J. Mater. Chem. A* 6, 16920–16931. doi: 10.1039/C8TA05291C

Wu, M.-C., Liao, Y.-H., Chan, S.-H., Lu, C.-F., and Su, W.-F. (2018b). Enhancing organolead halide perovskite solar cells performance through interfacial engineering using Ag-doped TiO_2 hole blocking layer. *Solar RRL* 2:1800072. doi: 10.1002/solr.201800072

Yang, B., Mahjouri-Samani, M., Rouleau, C. M., Geohegan, D. B., and Xiao, K. (2016). Low temperature synthesis of hierarchical TiO_2 nanostructures for high performance perovskite solar cells by pulsed laser deposition. *Phys. Chem. Chem. Phys.* 18, 27067–27072. doi: 10.1039/C6CP02896A

Zhang, J., Hultqvist, A., Zhang, T., Jiang, L., Ruan, C., Yang, L., et al. (2017). Al_2O_3 underlayer prepared by atomic layer deposition for efficient perovskite solar cells. *ChemSusChem* 10, 3810–3817. doi: 10.1002/cssc.201701160

Zhang, P., Wu, J., Zhang, T., Wang, Y., Liu, D., Chen, H., et al. (2018). Perovskite solar cells with ZnO electron-transporting materials. *Adv. Mater.* 30:1703737. doi: 10.1002/adma.201703737

Zhou, L., Chang, J., Liu, Z., Sun, X., Lin, Z., Chen, D., et al. (2018). Enhanced planar perovskite solar cell efficiency and stability using a perovskite/PCBM heterojunction formed in one step. *Nanoscale* 10, 3053–3059. doi: 10.1039/C7NR07753J

Conflict of Interest Statement: The authors declare that the research was conducted in the absence of any commercial or financial relationships that could be construed as a potential conflict of interest.